Climate Inferences from a Glaciological Reconstruction of the Late Pleistocene Wind River Ice Cap, Wind River Range, Wyoming

Author(s): Sean D. Birkel, Aaron E. Putnam, George H. Denton, Peter O. Koons, James L. Fastook, David E. Putnam and Kirk A. Maasch

Source: Arctic, Antarctic, and Alpine Research, 44(3):265-276. 2012.
Published By: Institute of Arctic and Alpine Research (INSTAAR), University of Colorado
DOI: http://dx.doi.org/10.1657/1938-4246-44.3.265
URL: http://www.bioone.org/doi/full/10.1657/1938-4246-44.3.265

Arctic, Antarctic, and Alpine Research, Vol. 44, No. 3, 2012, pp. 265–276

Climate Inferences from a Glaciological Reconstruction of the Late Pleistocene Wind River Ice Cap, Wind River Range, Wyoming

Sean D. Birkel@*
Aaron E. Putnam†*
George H. Denton‡*
Peter O. Koons‡*
James L. Fastook§*
David E. Putnam# and
Kirk A. Maasch‡*

*Climate Change Institute, University of Maine, Orono, Maine 04469, U.S.A.
†Lamont-Doherty Earth Observatory, Columbia University, Palisades, New York 10964, U.S.A.
‡Department of Earth Sciences, University of Maine, Orono, Maine 04469, U.S.A.
§Department of Computer Sciences, University of Maine, Orono, Maine 04469, U.S.A.
#School of Science and Mathematics, University of Maine at Presque Isle, Presque Isle, Maine 04769, U.S.A.
@Corresponding author: birkel@maine.edu

Abstract

We reconstructed the former ice cap of the Wind River Range, Wyoming, using a glaciological model with scaled modern temperature and precipitation inputs to examine probable climate during the local Last Glacial Maximum (LGM) (or Pinedale glaciation). A key result is that temperature anomalies of −10 °C, −8.5 °C, −6.5 °C, and −5 °C must compensate respective precipitation values of 50%, 100%, 200%, and 300% that of modern in order for the maximum glacier system to attain equilibrium. In further sensitivity tests, we find that ice-cap area and volume shrink by 75% under a climate forcing 50% modern and 50% LGM. The glacier system disappears altogether in ~100 years when subjected to sustained modern conditions. Our results are consistent with other interpretations of western U.S. LGM climate, and demonstrate that the Wind River Ice Cap could have disintegrated rapidly during the first phase of the termination. In future work we will simulate glacier-climate evolution as constrained by emerging ^{10}Be moraine chronologies.

DOI: http://dx.doi.org/10.1657/1938-4246-44.3.265

Introduction

The precise mechanisms through which Earth's climate system oscillates from glacial to interglacial modes of operation in response to insolation forcing remain poorly understood (Schaefer et al., 2006). To further explain the cause of ice ages, it is important to acquire detailed information about the past distribution of climate anomalies across the globe. Mountain glaciers are particularly sensitive to changes in temperature and precipitation (Oerlemans, 1989). First-order climate inferences are therefore commonly made from moraine records constraining the extent of former glaciers. Such inferences can be enhanced with the addition of a glaciological model, wherein the mass-balance history of a mapped glacier system is tested under independent variations of temperature and precipitation.

Here, we use one such model to develop a framework for investigating past glaciation and climate of the Wind River Range, Wyoming. This study is companion to an ongoing project evaluating interhemispheric climate change from the development of detailed ^{10}Be moraine chronologies for past glacier systems in New Zealand, South America, and the western U.S. (Schaefer et al., 2006; Putnam et al., 2010). Our objectives in this paper are twofold. The first objective is to reconstruct LGM ice thickness and extent across the Wind Rivers, and in doing so determine the range of temperature and precipitation anomalies under which the glacier system is sustained. For simplicity, we determine what temperature inputs must compensate precipitation values of 50%, 100%, 200%, and 300% that of modern. The second objective is to evaluate the sensitivity of the ice cap to climate change in scenarios of inception and decline. A future study will simulate the deglaciation of individual glaciers for comparison to new ^{10}Be moraine chronologies when the latter become available.

GEOLOGICAL SETTING AND GLACIATION OVERVIEW

The Wind River Range is a northwest-trending massif of late Archean granites and gneisses approximately 175 km long and 45 km wide in west-central Wyoming (Frost et al., 1998) (Fig. 1). The crest of the range forms the continental divide with 47 peaks above 4000 m elevation (Steidtmann et al, 1989). These peaks are flanked on the west by a scoured upland plateau (~3000 m), and to the east by a higher non-scoured surface (~3700 m) incised by deep U-shaped canyons. These and other erosional features of the range, including lake basins and the prominent ''hook'' in the upper Green River Valley, formed beneath an ice cap that grew and collapsed repeatedly throughout the late Quaternary period (Frost et al., 1998). We call this recurrent glacier system the *Wind River Ice Cap*. Modern glaciation is limited to small snowdrift-fed glaciers and perennial snowfields found in cirques below the range crest, most notably in the vicinity of Gannett Peak (Krimmel, 2002).

1523-0430/6 $7.00

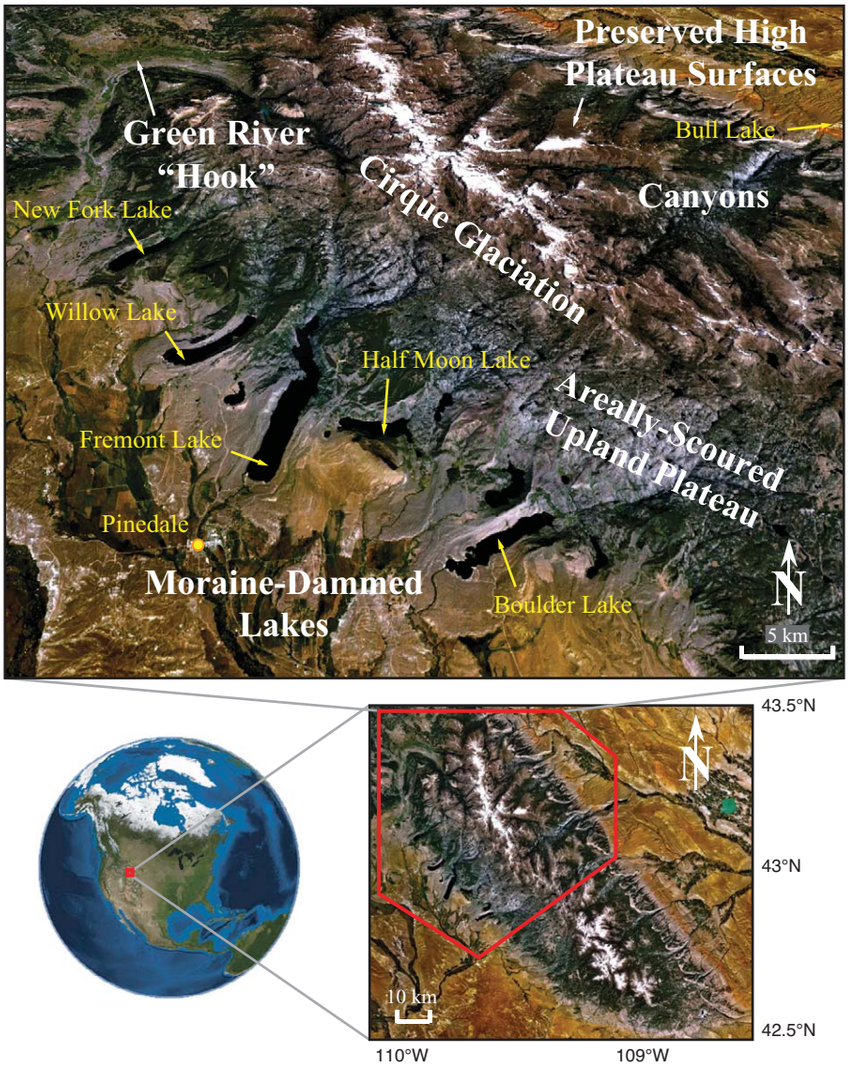

FIGURE 1. Wind River Range location map. Important features discussed in the text are identified. In color online.

Several large lake basins scoured by paleo–ice tongues along the western and eastern fronts of the Wind River Range are dammed by massive terminal moraines. Two such basins, Fremont Lake and Bull Lake, are the type localities for the Pinedale (marine isotope stage [MIS] 2) and Bull Lake (MIS 6) glacial units correlated throughout the Rocky Mountains (Blackwelder, 1915; Richmond, 1986). Existing cosmogenic ^{10}Be and ^{36}Cl exposure-age chronologies constrain the deposition of Pinedale moraines to 16–22 kyr BP, and Bull Lake moraines to 100–130 kyr BP (Gosse et al., 1995a; Phillips et al., 1997). It is noteworthy that Bull Lake moraines are found consistently outboard to Pinedale moraines, thus the Wind River Ice Cap was slightly more expansive during the MIS 6 glacial maximum than it was during that of MIS 2. Evidence of younger and more limited glaciation is found in high cirques far inboard to Pinedale moraines. Here, small weathered moraine belts, ascribed to the Temple Lake glaciation, lie downslope of modern glaciers and fresh historical-age moraines (Moss, 1951). Radiocarbon ages from sediments near Temple Lake and cosmogenic exposure ages from moraines in the Titcomb basin constrain the age of the Temple Lake glaciation to 11–14 kyr BP (Zielinski, 1989; Gosse et al., 1995b), making this glacial advance roughly coeval with the North Atlantic Younger Dryas event (e.g., Mayewski et al., 1993).

For simplicity, throughout the remainder of this paper we refer to the Pinedale stade as the local LGM, or just LGM.

PREVIOUS CLIMATE INFERENCES

The distribution of climate anomalies and the timing of maximum glaciation vary significantly across the western U.S.A. (Thackray, 2008). This complexity likely stems from circulation induced by the orography of the Laurentide and Cordilleran ice sheets in which storm tracks and the upper-level westerlies were shifted to the south relative to present mean positions (Antevs, 1948; Benson and Thompson, 1986). General circulation models (GCMs) indicate that annual average temperature across the American cordillera may have declined up to 10 °C, commensurate in some places with a significant increase in precipitation (Bartlein et al., 1998; Kutzbach et al., 1998; Bromwich et al., 2005).

In the Great Basin, expansive pluvial lakes formed during glacial stadials (Gilbert, 1890; Oviatt, 1997). Studies of these paleolakes yield annual temperature estimates similar to those predicted

by GCMs. For example, Kaufman (2003) estimated an LGM cooling of 7–13 °C from amino acid paleothermometry on fossil ostracodes collected from Lake Bonneville deposits. Likewise, a summer temperature depression of 7–9 °C across the Lake Bonneville basin was found in a hydrologic modeling study by Hostetler et al. (1994). It remains unclear whether the lakes expanded in response to severe summer temperature depression and weak effective evaporation (Kaufman, 2003), or from modest temperature depression and increased precipitation (Oviatt, 1997; Hostetler et al., 1994).

Glaciers underwent considerable expansion throughout the western U.S.A. during the LGM. Paleosnowline reconstructions, wherein glacier mass-balance change is assumed to be driven by mostly temperature, suggest greater than 10 °C cooling across much of the Rocky Mountains (Porter et al., 1983). Other studies in the region tested a variety of climate scenarios ranging from cool and wet to cold and dry. For example, Leonard (2007) found, using a mass balance model, that glaciation in Colorado and Wyoming could be induced by climate cooling ranging 3.5–10 °C commensurate with respective precipitation changes of double to half that of modern. It was also noted that precipitation enhancements from a Lake Bonneville moisture source seemed likely for the Wasatch Range and Uinta Mountains. Similar results for the latter two areas were found in glaciological reconstructions (Laabs et al., 2006; Refsnider et al., 2008).

Here, we use a glaciological model of the Wind River Range to test scenarios of ice-cap inception and decline, and to determine what LGM temperature anomalies would compensate precipitation values of 50%, 100%, 200%, and 300% relative to modern climate. Our methodology is comparable to the approaches of Leonard (2007), Laabs et al. (2006), and Refsnider et al. (2008) in that we attempt to simulate the glacier system under a range of physically plausible climates. In the next section we describe the glaciological model and climatology/mass-balance formulation, and then present results from the ice-cap reconstruction experiments.

Methods

THE GLACIOLOGICAL MODEL

We reconstructed the Wind River Ice Cap using the University of Maine Ice Sheet Model (UMISM) (Fastook and Prentice, 1994; Kleman et al., 2002; Naslund et al., 2003; Hooke and Fastook, 2007; Fastook et al., 2008). UMISM is a 2D finite element ice dynamics solver with embedded components for calculating isostasy, thermodynamics, basal water production and sliding, and surface mass balance (see Appendix for details). The force balance in UMISM follows the Shallow Ice Approximation (SIA) method (Hutter, 1983) in which longitudinal stresses are neglected for computational efficiency. Although models of this sort are used most widely for simulating ice sheets, they are also capable of simulating kilometer-scale ice caps and outlet glaciers (Le Meur and Vincent, 2003; Le Meur et al., 2004; Leysinger Vieli and Gudmundsson, 2004; Schäfer et al., 2008). SIA models comparable to UMISM have been used to study paleoglacier systems in the Wasatch and Uinta mountains, Utah, ~300 km southwest of the Wind River Range (Laabs et al., 2006; Refsnider et al., 2008).

Primary input to UMISM is a 0.8 km bedrock topography of the Wind River Range (resampled from a 30 m SRTM DEM) arranged in a quadrilateral grid of nodal points. A domain resolution of just under 1 km was chosen in order to resolve valleys and cirques, while minimizing SIA discrepancy from steep bedrock surface slopes (e.g., Le Meur et al., 2004). The input topography includes existing ice surfaces. Given that all modern glaciers within the Wind Rivers are positioned near the range crest and <2.5 km in length, we assume negligible impact of their topographies on the maximum ice-cap solution in which major flowlines extend 20–60 km.

Baseline climate in the model is defined from gridded input consisting of monthly mean temperature and total precipitation. We use a 1 km 1971–2000 climatology from PRISM (Parameter-elevation Regressions on Independent Slopes Model) (Daly et al., 1997) (Fig. 2). PRISM is a knowledge-based system that uses point measurements of temperature, precipitation, and other parameters to produce realistic gridded estimates of surface climate conditions. The PRISM data set is particularly robust over mountainous terrain, and thus ideal for our study of the Wind River Range. Past climate is approximated from the modern baseline by applying temperature and precipitation departure values, T and P. For example, $T = -3\,^{\circ}C$ implies a 3 °C cooling of the temperature seasonal cycle, and $P = 200\%$ implies a doubling of precipitation. The temperature field is modified by ice topography using a fixed vertical lapse rate of −6 °C/km, a value chosen as a reasonable fit to the altitudinal distribution of mean annual temperature observed in the PRISM climatology (Fig. 3). For simplicity, we assume that the pattern of temperature and precipitation remains largely the same between modern and past climate on the scale of a single mountain range such as the Wind Rivers. We nevertheless acknowledge that in reality there would be localized climate anomalies developing from the orography and albedo of the ice cap.

The climate signal at each gridpoint is transferred to the ice-flow solver through a calculation of net annual surface mass balance, or the difference between snow/ice accumulation and ablation. The mass-balance calculation is made using a degree day method similar to that of Braithwaite and Olesen (1989). Our algorithm first determines annual snow accumulation, which is done by summing precipitation amounts for all months when the temperature, T_{month}, is ≤0 °C. Precipitation is ignored for months when $T_{month} > 0$ °C. Likewise, when the latter condition is true the module also calculates the number of melting degrees (md) ($md_{month} = T_{month}$ − number of days in month), and then finds the annual total. Annual ablation is found by reducing accumulated snow at a prescribed snow melt rate, and then, if melting degrees remain, reducing a hypothetical column of ice at a prescribed ice melt rate. We use melt rates of 3 and 8 mm/md (water equiv.) for snow and ice, respectively, obtained from the mass-balance calibration described below.

MODEL CALIBRATION

Ice sheet models such as UMISM have changeable parameters that control some environmental conditions and flow characteristics of ice. In order to produce meaningful paleoglacier reconstructions, it is necessary to first tune the model so that output is consistent with existing observational data.

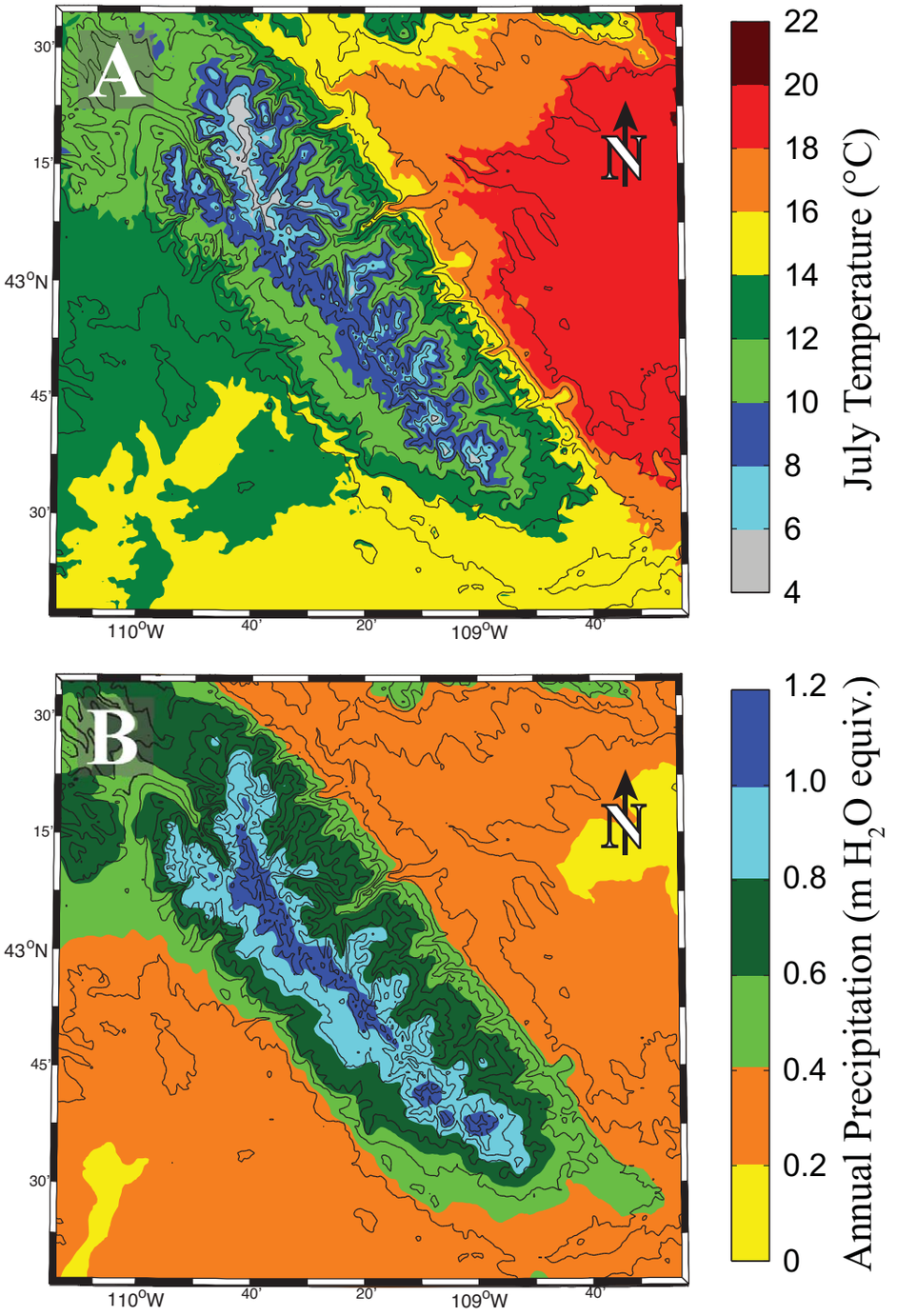

FIGURE 2. Example PRISM climatology input fields. A) Mean July temperature, and B) total annual precipitation. In color online.

Key changeable parameters in UMISM are the degree-day factors, namely the snow and ice melt rates used to calculate surface mass balance. Ideally, optimum values for these factors would be determined by matching observed and modeled snow cover calculated from the 1971–2000 PRISM climate baseline. However, existing glaciers and perennial snowfields in the Wind River Range are out of equilibrium with modern climate, and few snow accumulation areas remain. To surmount this problem, we conducted degree-day tests under preindustrial climate, which we assume is characterized by T = −1.5 °C and P = 100%. Given these conditions, we found optimal ablation rates of 3 and 8 mm/md for snow and ice, respectively, that afforded positive mass balance on the high plateau in areas recently deglaciated or now covered by wasting ice (Figs. 4, 5). A test case wherein the snow melt rate was increased to 5 mm/md failed to generate perennial snow, and required additional lowering of T to −2.6 °C in order to match the

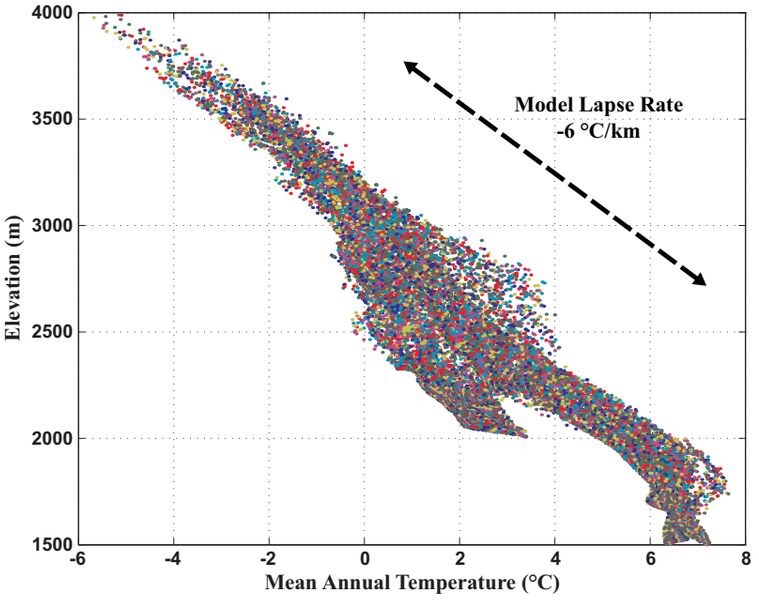

FIGURE 3. Plot of PRISM mean-annual temperature vs. elevation for the model domain. The temperature field is adjusted to ice topography at each model integration using a fixed vertical lapse rate of −6 °C/km. From the plot it is evident that lapse rate varies with altitude, and that there may be distinct populations. For example, the lapse rate from 2000 to 3000 m is ~4 °C/km, whereas from 3000 to 4000 m the value is ~6.5 °C/km. In color online.

favorable result of the first experiment. Degree-day factors vary significantly across different geographical settings, but range generally from 3 to 5 mm/md for snow ablation, and 6 to 8 mm/md for ice ablation (Braithwaite, 2011). In the absence of melt rate measurements specific to the Wind Rivers, we assume for now that our values are at least reasonable.

Ice-flow parameters tuned for this study include the sliding law constant, *B*, and flow enhancement factor, *E* (see Appendix for details). The value of *B* can be adjusted to either lessen or increase the amount of basal sliding due to melting and refreezing over rough beds. Low values of *B* afford relatively thin, fast flowing ice, whereas high values of *B* afford the opposite. Likewise, the value of *E* also can be changed in order to modify the thickness and flow of ice. In this case, *E* affects the ice hardness, and the values can be changed to reflect ice impurities. High values of *E* afford relatively stiff ice (resulting in greater thickness), and low values afford relatively soft ice (resulting in lesser thickness). Both sliding and ice-hardness parameters carry a temperature dependence.

Adjusting *B* and *E* provides a means to match modeled ice surfaces to existing geomorphological features under known climate conditions. Ideally, such experiments would be carried out for existing glaciers within the study domain for which the spatial extent, thickness, bed topography, velocity structure, and surface mass balance are measured quantities. However, as stated already, we are unable to conduct modern climate experiments in this study because of a lack of glacier bottom topography, and because the SIA method is unreliable for steep bed slopes in cirques where existing glaciers are found. We instead ran a suite of LGM ($T = -6.5$ °C; $P = 200\%$) simulations in which initial parameter values were taken from sensitivity tests of the Greenland Ice Sheet (Pingree, 2010). The parameters *B* and *E* were then adjusted (to 0.02 and 1, respectively) so that the surface altitudes of major outlet glaciers nearly equaled the altitudes of abutting lateral moraines, while the glacier termini extended to Pinedale moraines. Given this calibration bias, we emphasize that our results reported in the next section are internally consistent, but there is some uncertainty in what baseline LGM climate would produce the Wind River Ice Cap.

Results

EXPERIMENT 1

In this experiment, we determined from a series of equilibrium simulations what LGM temperature anomalies must compensate precipitation regimes of 50%, 100%, 200%, and 300% that of modern to sustain the maximum Wind River Ice Cap (Table 1; Fig. 6). A target LGM configuration for the glacier system was established by comparing output from initial simulations to the ice-cap footprint delineated by terminal moraines (Figs. 7, 8). The ''best fit'' to mapped features across the range is obtained when total ice area and volume is approximately 5.4×10^3 km^2 and 9×10^2 km^3, respectively. This fit includes the extension of most outlet glaciers to LGM terminal moraines. One notable exception is the piedmont lobe of the Green River outlet glacier, which in our model consistently grows beyond inferred LGM limits. Temperature departure values affording the target ice cap configuration are -5 °C ($P = 300\%$), -6.5 °C ($P = 150\%$), -8.5 °C ($P = 100\%$), and $T = -10$ °C ($P = 50\%$).

EXPERIMENT 2

In this experiment, we simulated two hypothetical scenarios of ice-cap evolution and assessed sensitivity of the maximum glacier system to extreme climate change. First, simulations were run using a sinusoidal climate forcing with a period of 2500 model years (Fig. 9). The temperature and precipitation signals in this simulation were coupled such that temperature decline was accom-

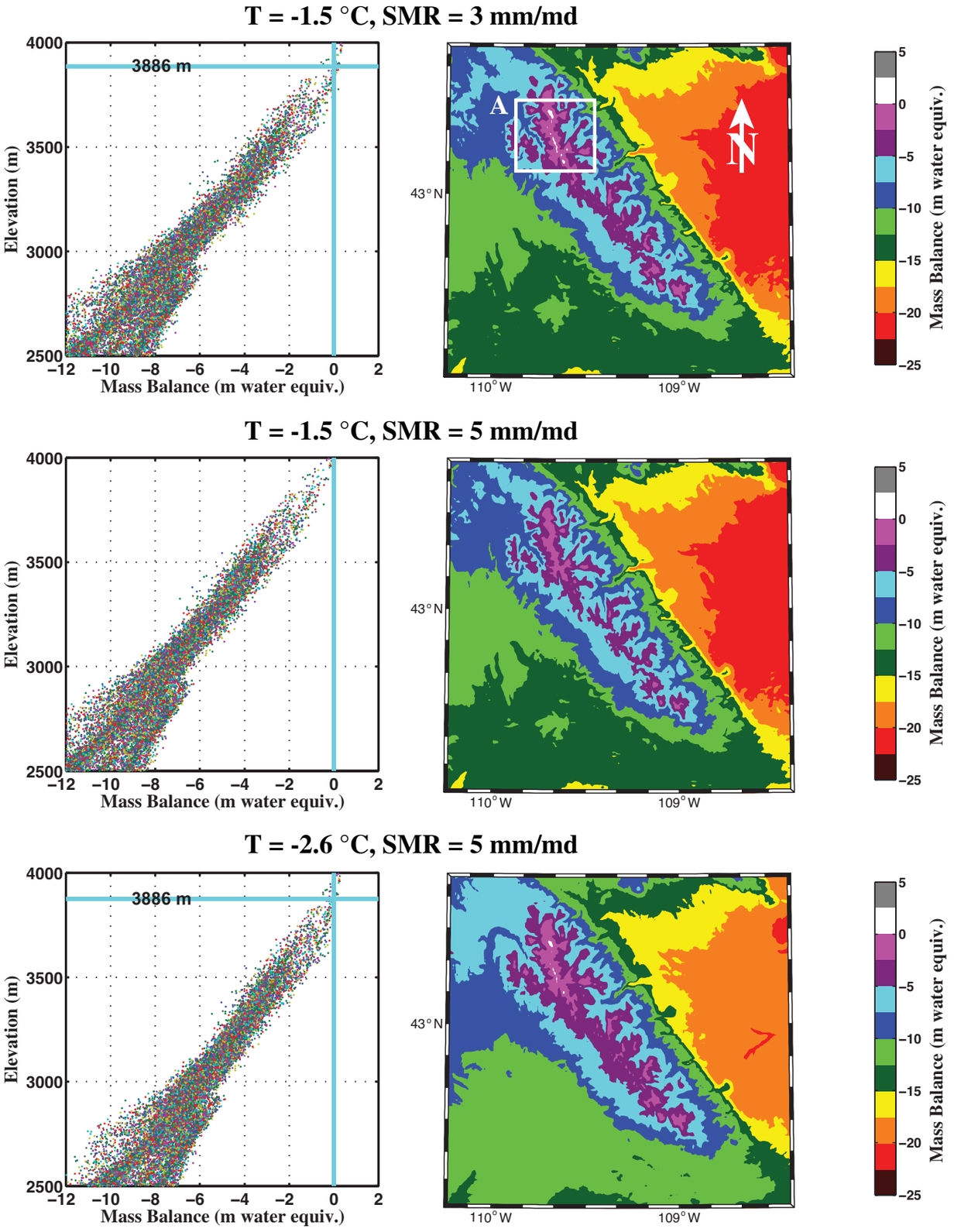

FIGURE 4. Mass-balance calibration results for two cases wherein the snow melt rate (SMR) was adjusted: T = −1.5 °C and SMR = 3 mm/md (top), T = −1.5 °C and SMR = 5 mm/md (middle), and T = −2.6 °C and SMR = 5 mm/md (bottom) (md = melting degrees). The first case generates snow cover over the high plateau consistent with observation. The mass balance vs. elevation plots in the left column include blue lines indicating the position of snowline. Increasing the SMR from 3 to 5 mm/md requires a 1.1 °C cooling compensation in order to attain equivalent snowline. The box labeled A in the top-right panel shows the area enlarged in Figure 5. In color online.

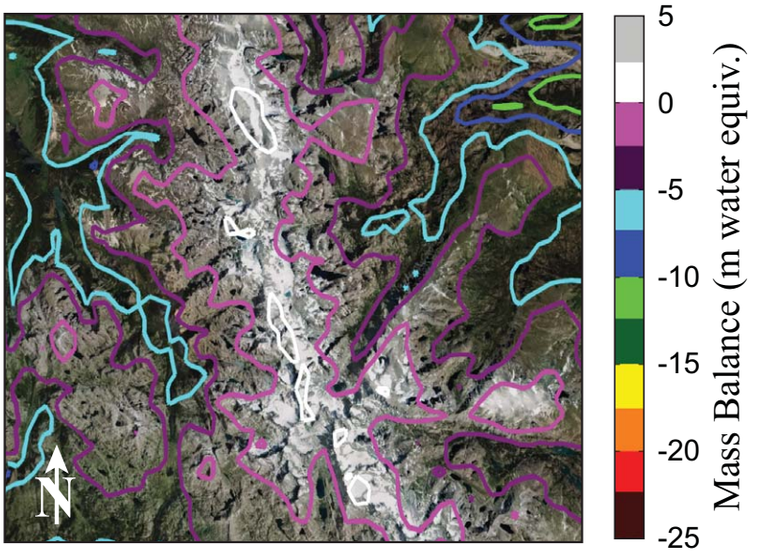

FIGURE 5. Contours of predicted mass balance overlain onto Google Earth™ imagery showing late summer snow cover and wasting ice caps on the high plateau of the northern Wind River Range. Shown here are results for T = −1.5 °C and snow melt rate = 3 mm/md. In color online.

modated by precipitation rise, and vice versa. The T and P maxima correspond to LGM climates tested in Experiment 1. We chose the arbitrary scenarios T = −5 °C and P = 250%, and T = −6 °C and P = 200%. The gray vertical lines at 500 and 2000 model years in Figure 9 mark when climate forcing is 50% modern and 50% LGM. The latter appears to be what one might consider a climate sensitivity threshold. During the ice-growth phase, temperature and precipitation conditions must exceed 50% that of LGM for any substantial increase in ice area and volume. Likewise, during the ice-decay phase, the ice cap shrinks by about 75% by the time climate conditions are halfway between modern and LGM. Based on the time difference between signal inflection points, ice-cap response lags the climate forcing by about 250 years during buildup, and by less than 200 years during decline. Finally, for the second part of this experiment, we subjected the LGM ice cap reconstructed above (T = −6 °C and P = 200%) instantaneously to sustained modern climate and found that it disappeared within ~100 years (Fig. 10).

Discussion

The first suite of glaciological reconstructions in this study highlight local climate conditions under which the LGM Wind River Ice Cap could form (Table 1; Figs. 6, 7, 8). We find a threefold increase in precipitation relative to that of modern must be compensated by a modest 5 °C temperature depression. Likewise, a doubling of precipitation requires a commensurate 6.5 °C cooling. In the case wherein precipitation remains effectively modern, a relatively severe temperature decline of 8.5 °C is required. Last, an LGM climate 50% drier than that of present needs to encompass a temperature cooling of about 10 °C in order for the ice cap to form. These results fit well within the range of climates predicted by previous studies (e.g., Antevs, 1948; Porter et al., 1983; Kutzbach et al., 1998; Leonard, 2007), and provide a means to further constrain the LGM temperature anomaly across the region if robust information about the precipitation signal could be obtained.

Results from the second experiment suite reveal additional information about the climatic sensitivity of the Wind River Ice Cap. Namely, the ice cap itself, as distinguished from unconnected cirque glaciers, forms only when climate across the region is at least halfway between that of modern and LGM (Fig. 9). Under such conditions, the range supports an ice cap only ~15% its LGM size in terms of area and volume. Total ice cover across the range appears to be impacted strongly by the intersection of snowline with upland plateaus above 3000 m, the latter which constitute broad accumulation areas. Given this mass-balance threshold, it is

TABLE 1

Summary of total ice area and volume attained by the end of each simulation in Experiment 1. Values in boldface correspond to ''best-fit'' simulations discussed in the text and highlighted in Figure 7.

$\times 10^3$ km^2/ $\times 10^2$ km^3	P = 50%	P = 100%	P = 150%	P = 200%	P = 250%	P = 300%
T = −5 °C	—	—	—	—	4/5.8	**5.3/8.7**
T = −6 °C	—	—	—	4.6/7.2	5.9/10	**—**
T = −6.5 °C	—	—	—	**5.5/9.4**	**—**	**—**
T = −7 °C	—	—	4.9/7.8	6.4/11.2	—	—
T = −8 °C	—	4.6/7.2	6.5/11.8	—	—	—
T = −8.5 °C	—	**5.5/9.2**	—	—	—	—
T = −9 °C	—	6.4/11.1	—	—	—	—
T = −10 °C	**5.2/8.5**	—	—	—	—	—

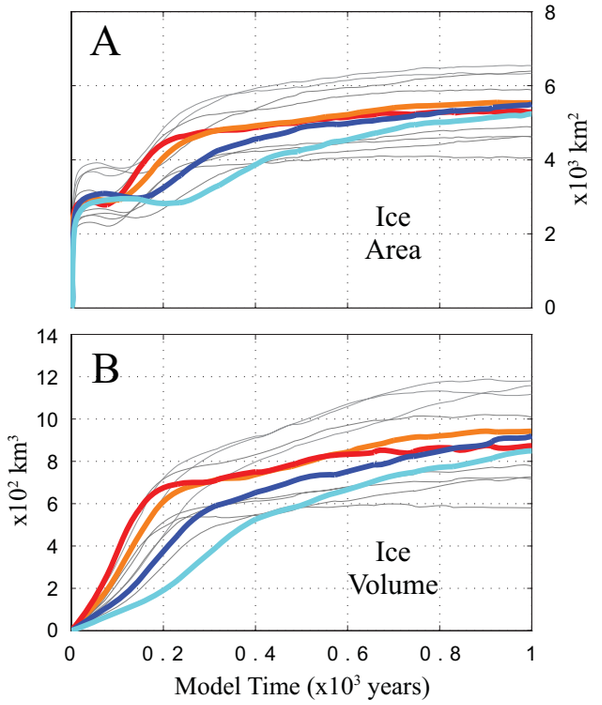

FIGURE 6. Experiment 1 time series stack showing results for (A) ice area and (B) ice volume. Key simulations are colored with heavyset lines: T = −5 °C and P = 300% (red); T = −6.5 °C and P = 200% (orange); T = −8.5 °C and P = 100% (blue); T = −10 °C and P = 50% (light blue).

not surprising to find in our experimentation that the glacier system shrinks rapidly during deglaciation, wherein the maximum ice cap is reduced 75% by the time climate is 50% modern and 50% LGM. We note the modeled glacier system is sensitive enough to detect decade-scale climate perturbations, which is important for matching changes in ice extent to high-precision ^{10}Be moraine chronologies (e.g., Schaefer et al., 2006; Putnam et al., 2010). In further assessing climatic sensitivity, we find from the extreme deglaciation scenarios that the maximum ice cap disintegrates in less than a century if subjected to sustained modern conditions. These results are consistent with evidence that the Wind River Ice Cap disappeared entirely during the first phase of the glacial termination (Gosse et al., 1995b), and emphasize the potential rapidity with which local ice caps can respond to climatic perturbations.

Our glaciological model of the Wind River Range has important shortcomings. The first is the inapplicability of the model to small existing glaciers on steep slopes near the range crest. This condition stems from the absence of longitudinal stresses in the force balance. We were therefore unable to calibrate UMISM in modern glacier simulations, and instead tuned the model in paleosimulations wherein ice thicknesses and extents were matched to moraines under a fixed LGM climate of T = −6.5 °C and P = 200%. Thus, although our results are internally consistent, there is some calibration bias. A second shortcoming is that our mass-balance calibration includes assumptions of preindustrial climate, as existing glaciers and snowfields are dwindling and not in equilibrium with present conditions. Further uncertainty arises from our choice of vertical lapse rate and degree-day factors used to translate the PRISM climatology to a surface mass balance. For example, changing the lapse rate from −6 to 7 °C/km would cause a drop in snowline and effective increase in the volume and extent of the ice cap. Even with these shortcomings, our glaciological reconstruction and climate interpretations are consistent with those of other studies, indicating to us that our model setup is at least reasonable.

Confidence in our Wind River Ice Cap reconstruction comes from the overall good fit between simulated ice extent and geomorphic features (refer to Figs. 1, 7, 8). In particular, most outlet glaciers in the model extend to LGM terminal moraines, including those of the Fremont Lake and Bull Lake drainages. Mapped features on the eastern side of the range appear to be best matched, with ice extending to inferred limits nearly everywhere. On the western side, all but two prominent glacier lobes extend to geomorphic targets. However, we note that on this side of the range, simulated ice on the upland plateau does not descend to margins deduced from areal bedrock scour. We suspect this deficiency arises because our climatology and mass-balance formulation uses modern precipitation grids that remain unmodified by ice orography (although temperature grids are modified using a lapse rate). In a more realistic climate treatment, precipitation should become relatively more concentrated along the ice margin due to orographic forcing as the ice cap expands. A similar conclusion was drawn from a simulation of the LGM Patagonian Ice Sheet (Sugden et al., 2002). Perhaps the most important mismatch between our model reconstruction and geomorphological data is that the piedmont lobe of the Green River outlet glacier consistently grows too large. Our suspicion is, again, that the unrealistic result stems from our simplified LGM climatology. The Green River outlet glacier was undoubtedly extensive enough to affect important local climate feedbacks that we cannot hope to capture in this study. In light of this, we will restrict future ^{10}Be moraine chronology comparisons to the smaller outlet glaciers draining east and west of the range divide that readily achieve steady state, namely the Fremont Lake and Bull Lake ice lobes.

Conclusions

We reconstructed the ice cap of the Wind River Range, Wyoming, using a glaciological model with robust mass balance in order to examine probable climate during the local LGM (or Pinedale stade) glaciation. This study constitutes the initial modeling framework that will be used to make climate inferences from detailed ^{10}Be moraine chronologies being developed for glacier systems in New Zealand, South America, and the western U.S.A. (Schaefer et al., 2006; Putnam et al., 2010). A key result here is that temperature anomalies of −10 °C, −8.5 °C, −6.5 °C, and −5 °C must compensate respective precipitation values of 50%, 100%, 200%, and 300% that of modern in order for the Wind River Ice Cap to attain an equilibrium configuration.

Further experimentation assessed the sensitivity of the ice cap to different scenarios of climatic change. We found that expansion and contraction of the ice cap is influenced strongly by intersection of snowline with upland plateau surfaces. For example, there is little ice cover across the range under climate less severe than 50%

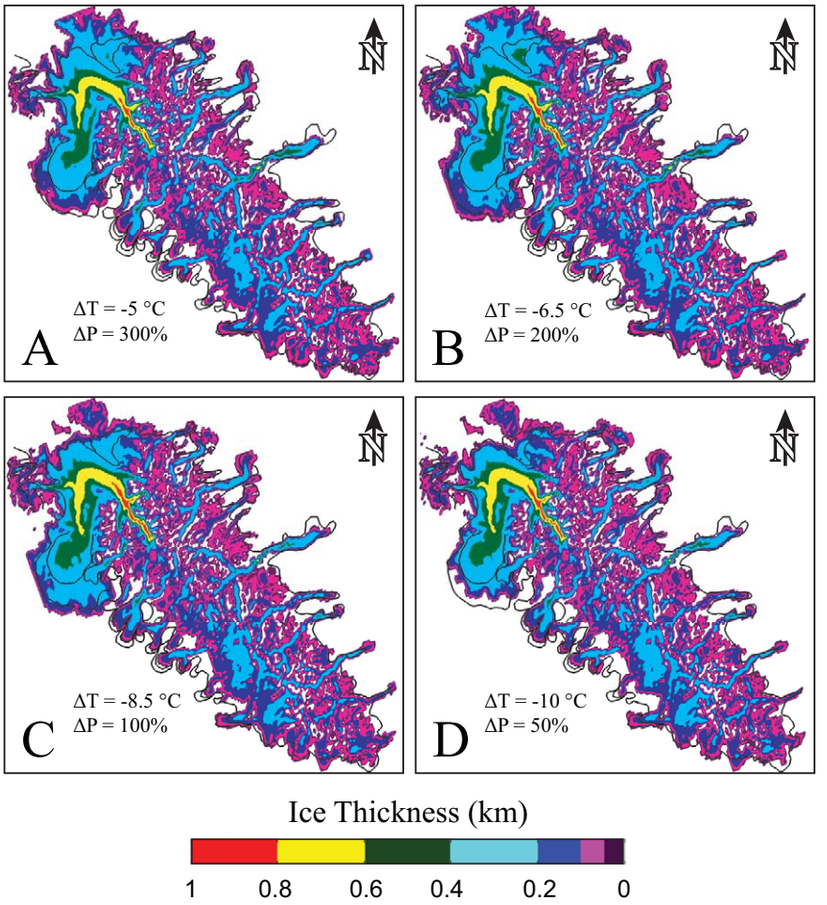

FIGURE 7. Ice thickness reconstructions for (A) T = −5 °C, P = 300%; (B) T = −6.5 °C, P = 200%; (C) T = −8.5 °C, P = 100%; and (D) T = −10 °C, P = 50%. Black outline denotes ice cap margin inferred from moraines. Areas in which there are two lines show Pinedale (inboard) and Bull Lake (outboard) margins. The greatest difference in ice thickness between the simulations is found over the Green River outlet glacier. Note the linear margins along the western side of the latter glacier in B and C delineate the edge of the model domain. Last Glacial Maximum (LGM) limits were inferred from Google Earth™ imagery with guidance from geomorphological interpretations in Gosse et al. (1995a, 1995b), and from unpublished fieldwork carried out in the summers of 2008 and 2009. In color online.

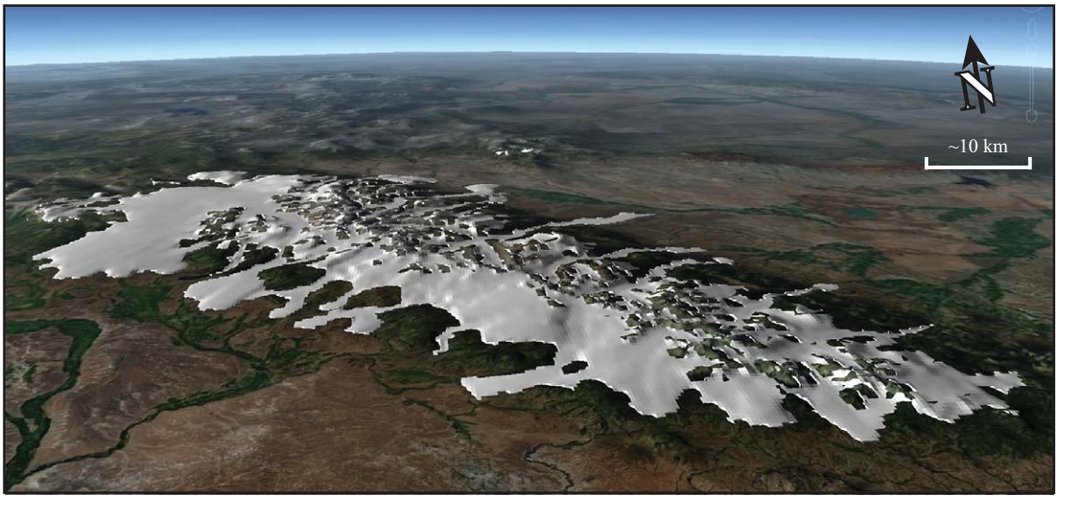

FIGURE 8. The LGM Wind River Ice Cap visualized as a shaded polygonal surface in Google Earth™. The solution shown is for T = −10 °C, P = 50%. In color online.

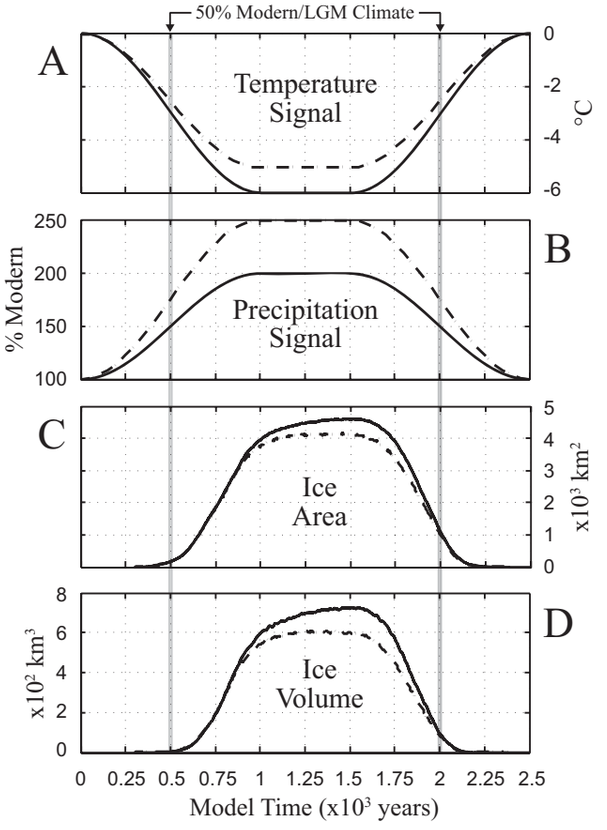

FIGURE 9. Experiment 2 time series stack. Shown are the (A) temperature and (B) precipitation forcing signals, and (C) ice area and (D) ice volume results for two climate scenarios. Solid lines correspond to T = −6 °C and P = 200%, and dashed lines correspond to T = −5 °C and P = 250%. Gray vertical lines highlight the model time at which the climate forcing is half-way between modern and LGM end members.

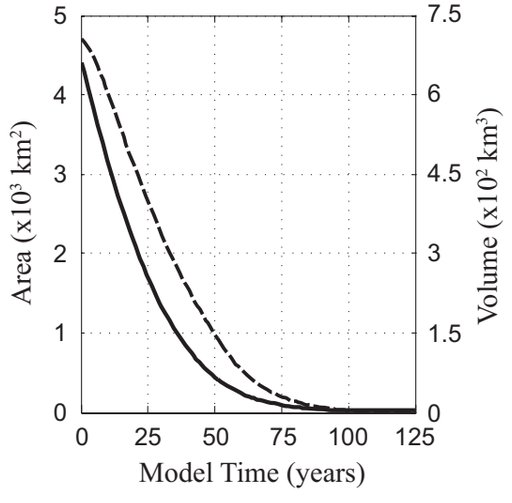

FIGURE 10. Experiment 2 deglaciation results. In this simulation, the LGM ice cap attained under a climate of T = −6 °C and P = 200% was subjected to sustained modern climate. The ice cap disintegrates in this extreme case within ~100 years.

modern and 50% LGM. Likewise the maximum glacier system shrinks by 75% under climate forcing 50% modern and 50% LGM. We also find from an extreme deglaciation scenario that the maximum ice cap disintegrates within ~100 years if subjected to sustained modern climate. The latter results are consistent with evidence that the Wind River Ice Cap disappeared during the first phase of the glacial termination (Gosse et al., 1995b).

We find good fit overall between the reconstructed LGM Wind River Ice Cap and the footprint of the glacier system inferred from geomorphic features. In particular, most outlet glaciers in the model extend to LGM terminal moraines, including those of the Fremont Lake and Bull Lake drainages. The most important mismatches with geomorphic data are too little ice in places along the western ice cap margin, and the extension of the piedmont lobe of the Green River outlet glacier beyond LGM targets. We suspect these deficiencies arise because our climatology and mass-balance formulation uses modern precipitation grids that are not modified by ice orography. Given the many assumptions in our experiment setup, we must also consider problems related to the SIA method, ice-flow calibration, or our choices of vertical lapse rate and degree-day factors.

Future work will expand upon this study in at least three ways. First, we will further calibrate the UMISM sliding and ice hardness parameters in sensitivity tests conducted for individual basins. The calibration used in this study is adapted from one conducted for the Greenland Ice Sheet (Pingree, 2010), and focuses more broadly on model-geomorphic fits across the range. Second, we will generate an LGM climatology for the Wind River Range using a dynamical mesoscale weather and climate model with LGM surface topography from this study. The resultant temperature and precipitation fields will include the effects of ice orography, and thus will provide robust input to the UMISM model mass-balance solver. Improved mass balance might resolve, for example, the problem of the Green River ice lobe growing too large in comparison to other outlet glaciers. Last, we plan to use the model framework developed here to simulate the retreat and ice-climate coupling of individual glaciers during the last termination. The latter experimentation will be constrained by emerging ^{10}Be moraine chronologies (e.g., Schaefer et al., 2006; Putnam et al., 2010).

Acknowledgments

We are grateful for funding of this work provided by the National Science Foundation (ITEST-0737583, EAR-1009626), Comer Science Foundation, and the Quesada Family Foundation. Three anonymous reviewers provided thoughtful suggestions that improved this manuscript. Sean Birkel would also like to thank his postdoctoral mentor Dr. Paul Mayewski for guidance and support.

References Cited

Antevs, E., 1948: Climatic changes and pre-white man: *In* Blackwelder, E., Hubbs, C. L., and Antevs, E. (eds.), The Great Basin, with Emphasis on Glacial and Postglacial Times. Salt Lake City: *University of Utah Bulltein*, 38(20): 168–191.

Bartlein, P. J., Anderson, K. H., Anderson, P. M., Edwards, M. E., Mock, C. J., Thompson, R. S., Webb, R. S., Webb, T., III, and Whitlock, C., 1998: Paleoclimate simulations for North America

over the past 21,000 years: features of the simulated climate and comparisons with paleoenvironmental data. *Quaternary Science Reviews*, 17: 549–585.

Benson, L. V., and Thompson, R. S., 1986: Lake-level variation in the Lahontan Basin for the past 50,000 years. *Quaternary Research*, 28: 69–85.

Blackwelder, E., 1915: Post-Cretaceous history of the mountains of central and western Wyoming, Part III. *Journal of Geology*, 23(4): 307–390.

Braithwaite, R. J., 2011: Why do we expect glacier melting to increase under global warming? *In* Blanco, J., and Kheradmand, H. (eds.), *Climate Change–Geophysical Foundations and Ecological Effects*. InTech, 520 pp., http://www.intechopen.com/books/climate-change-geophysical-foundations-and-ecological-effects.

Braithwaite, R. J., and Olesen, O. B., 1989: Calculation of glacier ablation from air temperature, West Greenland. *In* Oerlemans, J. (ed.), *Glacier Fluctuations and Climate Change.* Dordrecht: D. Reidel Publishing Company, 160 pp.

Bromwich, D. H., Toracinta, E. R., Oglesby, R. J., Fastook, J. L., and Hughes, T. J., 2005: LGM summer climate on the southern margin of the Laurentide Ice Sheet: wet or dry? *Journal of Climate*, 18: 3317–3338.

Daly, C., Taylor, G., and Gibson, W., 1997: The PRISM approach to mapping precipitation and temperature. *In* American Meteorological Society: *10th Conf. on Applied Climatology, Reno, NV,* 10–12.

Fastook, J. L., and Prentice, M., 1994: A finite-element model of Antarctica: sensitivity test for meteorological mass-balance relationship. *Journal of Glaciology*, 40(134): 167–175.

Fastook, J. L., Head, J. W., Marchant, D. R., and Forget, F., 2008: Tropical mountain glaciers on Mars: altitude-dependence of ice accumulation, accumulation conditions, formation times, glacier dynamics, and implications for planetary spin-axis/orbital history. *Icarus*, 198: 305–317.

Frost, C. D., Frost, B. R., Chamberlain, K. R., and Hulsebosch, T. P., 1998: The Late Archean history of the Wyoming province as recorded by granitic magmatism in the Wind River Range, Wyoming. *Precambrian Research*, 89: 145–173.

Gilbert, G. K., 1890: Lake Bonneville: Washington, D.C.: *U.S. Geological Survey Monograph*, 1: 438 pp.

Glen, J. W., 1955: The creep of polycrystalline ice. *Proceedings of the Royal Society of London,* 228:519–538.

Gosse, J. C., Klein, J., Evenson, E. B., Lawn, B., and Middleton, R., 1995a: Beryllium-10 dating of the duration and retreat of the last Pinedale glacial sequence. *Science*, 268(5215): 1329–1333.

Gosse, J. C., Evenson, E. B., Klein, J., Lawn, B., and Middleton, R., 1995b: Precise cosmogenic ^{10}Be measurements in western North America: support for a global Younger Dryas cooling event. *Geology*, 23(10): 877–880.

Hooke, R. L., and Fastook, J. L., 2007: Thermal conditions at the bed of the Laurentide ice sheet in Maine during deglaciation: implications for esker formation. *Journal of Glaciology*, 53(183): 646–658.

Hostetler, S. W., Giorgi, F., Bates, G. T., and Bartlein, P. J., 1994: Lake-atmosphere feedbacks associated with paleolakes Bonneville and Lahontan. *Science*, 263: 665–668.

Hutter, K., 1983: *Theoretical Glaciology: Material Science of Ice and the Mechanics of Glaciers and Ice Sheets.* Dordrecht: D. Reidel Publishing Company; Tokyo: Terra Scientific Publishing Company, 510 pp.

Kaufman, D. S., 2003: Amino acid paleothermometry of Quaternary ostracodes from the Bonneville Basin, Utah. *Quaternary Science Reviews*, 22: 899–914.

Kleman, J., Fastook, J. L., and Stroeven, A. P., 2002: Geologically and geomorphologically constrained numerical model of Laurentide Ice Sheet inception and build-up. *Quaternary International*, 95/96: 87–98.

Krimmel, R. M., 2002: Glaciers of the western United States. *In* Williams, R. S., Jr., and Ferrigno, J. G. (eds.), *Satellite Image Atlas of Glaciers of the World.* Reston, Virginia: *U.S. Geological Survey Professional Paper*, 1386-J (Glaciers of North America): J360.

Kutzbach, J., Behling, P., Gallimore, R., Harrison, S., Laarif, F., and Selin, R., 1998: Climate and biome simulations for the past 21,000 years. *Quaternary Science Reviews*, 17: 473–506.

Laabs, B. J. C., Plummer, M. A., and Mickelson, D. M., 2006: Climate during the last glacial maximum in the Wasatch and southern Uinta Mountains inferred from glacier modeling. *Geomorphology*, 37: 300–317.

Le Meur, E., and Vincent, C., 2003. A two-dimensional shallow ice-flow model of Glacier de Saint-Sorlin, France. *Journal of Glaciology*, 49(167):527–538.

Le Meur, E., Gagliardini, O., Zwinger, T., and Ruokolainen, J., 2004: Glacier flow modelling: a comparison of the Shallow Ice Approximation and the full-Stokes solution. *Comptes Rendus Physique*, 5: 709–422.

Leonard, E., 2007: Modeled patterns of Late Pleistocene glacier inception and growth in the Southern and Central Rocky Mountains, USA: sensitivity to climate change and paleoclimatic implications. *Quaternary Science Reviews*, 26(17/18): 2152–2166.

Leysinger Vieli, G. J.–M. C., and Gudmundsson, G. H., 2004: On estimating length fluctuations of glaciers caused by changes in climatic forcing. *Journal of Geophysical Research*, 109: F01007, 558–559.

Mayewski, P. A., Meeker, L. D., Whitlow, S., Twickler, M. S., Morrison, M. C., Alley, R. B., Bloomfield, P., and Taylor, K., 1993: The atmosphere during the Younger Dryas. *Science*, 261(5118): 195–197.

Moss, J. H., 1951: Late glacial advances in the southern Wind River Mountains, Wyoming. *American Journal of Science*, 249: 865–883.

Naslund, J. O., Fastook, J. L., and Holmlund, P., 2003: New ways of studying ice sheet flow directions and glacial erosion by ice sheet modelling—Examples from Fennoscandia. *Quaternary Science Reviews*, 22(2/4): 89–102.

Oerlemans, J., 1989: On the response of valley glaciers to climate change. *In* Oerlemans, J. (ed.), *Glacier Fluctuations and Climate Change.* Dordrecht: D. Reidel Publishing Company, 160 pp.

Oviatt, C. G., 1997: Lake Bonneville fluctuations and global climate change. *Geology*, 25: 155–158.

Paterson, W. S. B., 1994: *The Physics of Glaciers*. 3rd edition. Oxford: Pergamon.

Phillips, F. M., Zreda, M. G., Gosse, J. C., Klein, J., Evenson, E. B., Hall, R. D., Chadwick, O. A., and Sharma, P., 1997: Cosmogenic ^{36}Cl and ^{10}Be ages of Quaternary glacial and fluvial deposits of the Wind River Range, Wyoming, *Geological Society of America Bulletin*, 109: 1453–1463.

Pingree, K., 2010: *The Greenland Ice Sheet: Reconstruction under Modern-Day Conditions and Sensitivity to the North Atlantic Oscillation*. M.S. thesis, Department of Earth Sciences, University of Maine, Orono.

Porter, S. C., Pierce, K. L., and Hamilton, T. D., 1983: Late Wisconsin mountain glaciation in the western United States. *In* Porter, S. C. (ed.), *Late-Quaternary Environments of the United States. Volume 1. The Late Pleistocene*. Minneapolis: University of Minnesota Press, 71–111.

Putnam, A. E., Denton, G. H., Schaefer, J. M., Barrell, D. J. A., Andersen, B. G., Finkel, R. C., Schwartz, R., Doughty, A. M., Kaplan, M. R., and Schlüchter, C., 2010: Glacier advance in southern middle-latitudes during the Antarctic Cold Reversal. *Nature Geoscience*, 3: 700–704.

Refsnider, K. A., Laabs, B. J. C., Plummer, M. A., Mickelson, D. M., Singer, B. S., and Caffee, M. W., 2008: Last Glacial Maximum climate inferences from cosmogenic dating and glacier modeling of the western Uinta ice field, Uinta Mountains, Utah. *Quaternary Research*, 69: 130–144.

Richmond, G. M., 1986: Stratigraphy and correlation of glacial deposits of the Rocky Mountains, the Colorado Plateau and the ranges of the Great Basin. *Quaternary Science Reviews*, 5: 99–127.

Schaefer, J. M., Denton, G. H., Barrell, D. J. A., Ivy-Ochs, S., Kubik,

P. W., Andersen, B. G., Phillips, F. M., Lowell, T. V., and Schlüchter, C., 2006: Near-synchronous interhemispheric termination of the Last Glacial Maximum in mid-latitudes. *Science*, 312: 1510–1513.
Schäfer, M., Gagliardini, O., Pattyn, F., and Le Meur, E., 2008: Applicability of the Shallow Ice Approximation inferred from model inter-comparison using various glacier geometries. *The Cryosphere* (Discussions), 2: 557–599.
Steidtmann, J. R., Middleton, L. T., and Shuster, M. W., 1989: Post-Laramide (Oligocene) uplift in the Wind River Range, Wyoming. *Geology*, 17: 38–41.
Sugden, D. E., Hulton, N. R. J., and Purves, R. S., 2002: Modelling the inception of the Patagonian icesheet. *Quaternary International*, 95/96: 55–64.
Thackray, G. D., 2008: Varied climatic and topographic influences on Late Pleistocene mountain glaciation in the western United States. *Quaternary Science*, 23(6/7): 671–681.
Weertman, J., 1964: The theory of glacier sliding. *Journal of Glaciology*, 5(39): 287–303.
Zielinski, Z. A., 1989: Lacustrine sediment evidence opposing Holocene rock glacier activity in the Temple Lake valley, Wind River Range, Wyoming, U.S.A. *Arctic and Alpine Research*, 21(1): 22–33.
MS accepted March 2012

Appendix

A complete description of UMISM can be found in Fastook and Prentice (1994) and Fastook et al. (2008). Here we provide only an overview of the model ice-flow solver in order to give context for the tuning reported in the methods section. The latter pertains to mainly the ice hardness and sliding parameters below in Equations (A2), (A3), and (A5).

The core of UMISM is a differential equation for ice extent and thickness as a function of time derived from an integrated momentum conservation equation based on the flow law of ice (Glen, 1955), coupled with a continuity equation for mass conservation:

$$\frac{\delta h}{\delta t} = MD - \nabla \cdot (UH), \tag{A1}$$

where $\delta h/\delta t$ is the time-dependent ice-surface elevation, MB is the net annual surface mass balance (accumulation minus ablation), U is the column-average ice velocity, and H is the ice thickness.

U in Equation (A1) is obtained by expanding:

$$\dot{\boldsymbol{\varepsilon}} = \left[\frac{\sigma}{A}\right]^n, \tag{A2}$$

which is a tensor equation expressing strain rates, $\dot{\boldsymbol{\varepsilon}}$, and stresses, σ, through a nonlinear power law. In this equation, n is the empirical flow law constant (we use a value of 3 for temperate glaciers [Paterson, 1994]), and A is a temperature dependent function that represents ice hardness in an Arrhenius relationship:

$$A = EA_0 e^{-Q/RT}, \tag{A3}$$

where A_0 is a constant, Q is the activation energy for ice creep, R is the gas constant, T is the ice temperature, and E is a tuning (or flow enhancement) parameter meant to account for ice impurities.

By shallow-ice approximation, all stresses and strain rates are ignored in the force balance except basal drag. Thus, the stress in Equation (A2) acting on the bed, or the ''driving'' stress, is expressed as:

$$\sigma_{xz} = \rho g H E \nabla h, \tag{A4}$$

where σ_{xz} is a stress in the x-direction acting on a surface with normal in the z-direction, ρ is density of ice, g is gravitational acceleration, H is ice thickness, and ∇h is ice-surface slope.

Finally, U, is calculated from the sum of velocity due to internal deformation, U_D, and velocity due to basal sliding, U_S, as expressed:

$$U = U_D + U_S = \frac{2}{n+2}\left[\frac{\rho g \nabla h}{A}\right]^n H^{n+1} + \left[\frac{\rho g \nabla h}{B}\right]^m H^m, \tag{A5}$$

where the last term follows a general sliding law relationship developed by Weertman (1964) for beds at the melting point. Here n is the empirical flow law constant in Equation (A2), A is the ice hardness parameter described in Equation (A3), B is the sliding law constant, and m is the sliding law exponent.